Role of Initial Vibrational and Rotational Reactant Excitation for the Reaction Dynamics of $H_2(\nu_0,J_0)$ with $Si^+(^2P)$

Nihed Chaâbane, Holger Vach,* and Pere Roca i Cabarrocas

Laboratoire de Physique des Interfaces et des Couches Minces, CNRS-Ecole Polytechnique, 91128 Palaiseau Cedex, France

Received: February 10, 2003; In Final Form: November 17, 2003

Molecular dynamics simulations with semiempirical quantum chemistry have been used to investigate the reaction dynamics of ground-state silicon ions with molecular hydrogen for translational impact energies between 0.5 and 10 eV. The validity of the employed PM3 method is demonstrated in comparison to high-level ab initio CCSD(T) calculations. Reaction cross sections for both $SiH^+(\nu,J)$ formation and complete dissociation are determined for different initial vibrational and rotational excitation states of the $H_2(\nu_0,J_0)$ molecules. Heating the commonly used room temperature hydrogen plasma to a maximum possible experimental value of 1000 K only results in a very modest increase of the reactive cross section for SiH^+ production by about 25%. The use of selective laser excitation of the reactants, however, permits us to increase the reactivity drastically. In this latter case, initial rotational laser excitation enhances the reactivity of our system as much as vibrational excitation, illustrating that only the amount of the initial excitation and not its precise nature influences the reaction dynamics. Furthermore, we show how the initial vibrational, rotational, and translational energies of the H_2 reactants control the final energy distributions of the SiH^+ products. The mechanisms leading to the observed reaction dynamics are discussed.

1. Introduction

The reaction dynamics of even small systems can be quite complicated because of numerous competing reaction paths.[1] Therefore, understanding how changes of the initial conditions affect the reaction dynamics and the product energy distributions has become an important question in physical chemistry. A variety of reactions has been investigated for this reason: either with various impact energies[2,3] or with initial electronic excitation of the reactants.[4,5]

In the present study, we focus on the reaction dynamics of molecular hydrogen $H_2(\nu_0,J_0)$ with silicon ions $Si^+(^2P)$ to form $SiH^+(\nu,J)$ or to dissociate completely. This reaction has evoked continuous interest for several reasons. First, the role of hydrogen atoms in semiconductor materials is very important to improve our understanding of nanotechnology devices.[6,7] For instance, hydrogen is known to passivate efficiently various surfaces as amorphous silicon by saturating dangling bonds. Those passivation reactions can radically change the electrical and optical properties of the involved devices. Second, the title reaction has become a model system to experimentally study the dynamics of ion−molecule reactions.[8] Finally, this reaction plays a significant role in chemical vapor deposition (CVD) of silicon in the electronic industry and even in astrophysics due to the existence of SiH^+ in interstellar space.[9]

Despite its apparent importance, the reaction kinetics of ionic silicon with molecular hydrogen has not been investigated in great detail. Experimentally, Armentrout et al. measured the reactive cross section of the title reaction.[8] In a recent theoretical work, trajectory calculations were performed at a hydrogen temperature of 305 K corresponding to the experimental conditions of Armentrout.[10] This temperature corresponds energetically to H_2 molecules in their vibrational ground state and in their first rotational state ($\nu_0 = 0$, $J_0 = 1$). The simulation results were in excellent quantitative agreement with the experimental findings for the reactive cross section σ as a function of relative impact energy E_0.[10,11] For the first time, it was shown under which conditions the reactants follow a direct or a complex-mediated reaction path.

For a room temperature hydrogen gas, the maximum reactive cross section was found to be limited to 1.64×10^{-16} cm^2 at a relative kinetic impact energy of 4 eV. In the present work, we therefore explore the question whether thermal heating of the hydrogen gas or selective laser excitation of the $H_2(\nu_0,J_0)$ reactants could possibly increase the reactivity of our system beyond the values previously found in experiments and numerical simulations.

2. Computational Details

We already demonstrated elsewhere that the semiempirical molecular orbital method PM3[12,13] yields energies and geometries of all intermediates and products for the reaction of Si^+ with H_2 in remarkable agreement with experiment and ab initio calculations.[10,11,14] However, a yet more convincing proof for the validity of our calculational method would be a direct comparison between the potential energy surfaces (PES) obtained from the PM3 method and from high-level ab initio calculation as, for instance, coupled cluster calculations as CCSD(T). Therefore, we present three different potential energy curves obtained with the GAUSSIAN 98 suite of programs[15] for the Si^+ interaction with atomic hydrogen in Figure 1. From simple inspection of this figure, we conclude that the semiempirical PM3 method yields Si^+−H interaction energies in good agreement with the results of high-level ab initio calculations. Especially, we like to underline that the equilibrium distance and the depth of the potential well are perfectly reproduced by

* Corresponding author. Fax: 00.33.1.69.33.30.06. E-mail: vach@leonardo.polytechnique.fr.

10.1021/jp034341l CCC: $27.50
Published on Web 02/11/2004

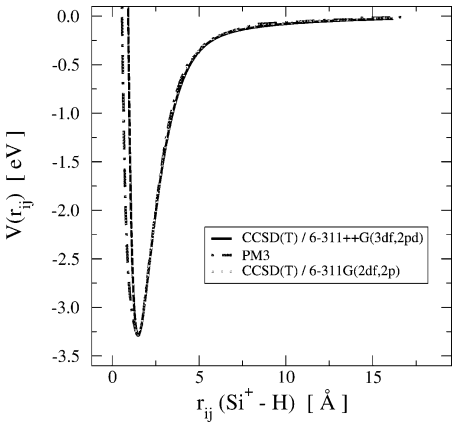

Figure 1. Potential energy curve for the SiH^+ molecule calculated with the semiempirical PM3 method in comparison to high-level ab initio CCSD(T) calculations (see text).

the two investigated methods; i.e., for all interatomic distances larger than 1.3 Å the two curves coincide quantitatively within about 1%. Only for interatomic distances shorter than 1.05 Å might the absolute potential energy values differ by as much as 1 eV, i.e., about one-third of the total potential well depth. For the present study, however, the fraction of atoms that approach each other that closely is less than about 5%. For realistic plasma reactor conditions (as for low-temperature PECVD), the situation becomes yet more favorable: we estimated that the portion of Si ions and H atoms that get closer to each other than about 1.3 Å is completely negligible; i.e., for those deposition plasma conditions, we expect that the PM3 potential values agree within 1 or 2% with those given by CCSD(T) calculations. In addition, we like to point out that the PES curves resulting from PM3 and CCSD(T) calculations presented in Figure 1 remain rather parallel even for very small distances. Consequently, the resulting interatomic forces are nearly identical due to the very comparable slopes, even for those very short interatomic distances. Only due to this similitude between the two PES curves was it possible to reproduce the experimental results by Armentrout et al. so well with the PM3 method.[10]

To demonstrate yet further the validity of the PM3 method for our present reaction system, we show the SiH_2^+ potential energy surface obtained from both ab initio CCSD(T) and semiempirical PM3 calculations in Figures 2 and 3, respectively. For both figures, a linear configuration between the three atoms was employed. Recalculating both PESs with a 120° angle defined among the three atoms, we again find two potential energy surfaces that are nearly identical. Due to the very satisfactory similarity between the two potential energy curves, we prefer in the following to profit from the advantages of a "direct dynamics" simulation using PM3 quantum chemistry instead of fitting the CCSD(T) PES. This choice becomes further sustained by the fact that the necessary PM3 simulations are not much more expensive to calculate than those with typical model potentials.

Consequently, all trajectories presented in the following are simulated using the semiempirical molecular orbital method PM3 to determine the interatomic potential energies at each time step. Our criterion for a converged, self-consistent field is that the total energy at two successive iteration steps differs by less than 10^{-9} kcal/mol. All trajectories are evaluated by solving the classical Newtonian equations of motion with the Venus-Mopac computer program[16] using a fifth-order Gear algorithm.[17] The time step of the numerical integration of these equations is

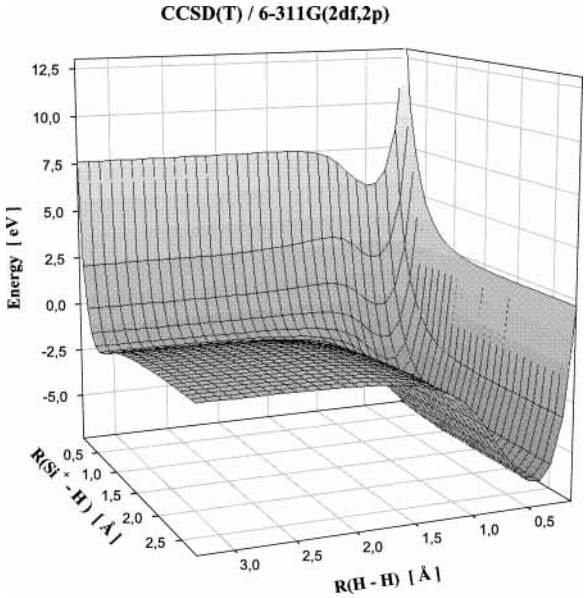

Figure 2. SiH_2^+ potential energy surface calculated with the high-level ab initio method CCSD(T) (see text).

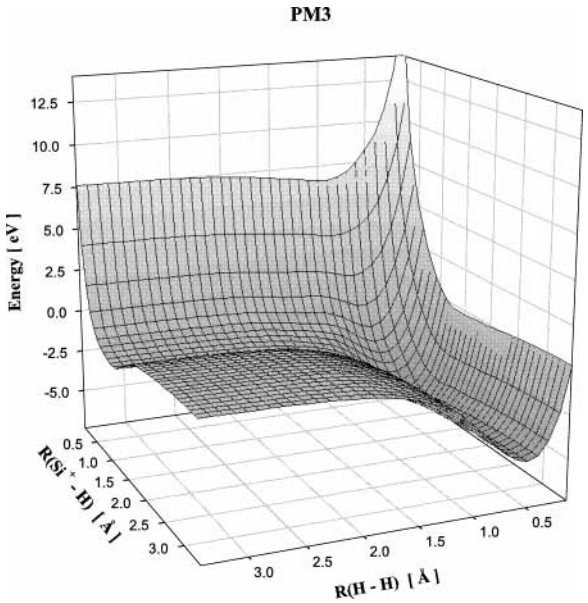

Figure 3. SiH_2^+ potential energy surface calculated with the semiempirical PM3 method (see text).

chosen to be 0.001 fs; all trajectories are followed over 3000 fs. For each impact energy E_0, between 100 and 500 trajectories are analyzed that all conserved their total energy to better than 1%. For each trajectory, the impact parameter b is randomly chosen between 0 and 1.5 Å and the impact energy is randomly sampled with a width of 10% around the investigated collision energy E_0.[14] A reaction is considered direct when only one inner turning point occurs, which corresponds to half a rotational period of the reaction complex.[18] For complex-mediated reactions, the complex lifetime τ is determined from the time interval between the first and the last turning point of the complex.

In the present work, we extend our previous study to H_2 molecules that are vibrationally and/or rotationally excited prior to their ion encounter and test the influence of their internal energy excitation on the $Si^+(^2P) + H_2(v_0,J_0) \rightarrow SiH^+(v,J) + H$ reaction. The collision energy E_0 and the initial internal energies E_{v_0,J_0} of the H_2 reactants are fixed at the beginning of each trajectory. Taking as reference the energy of the silicon ion and

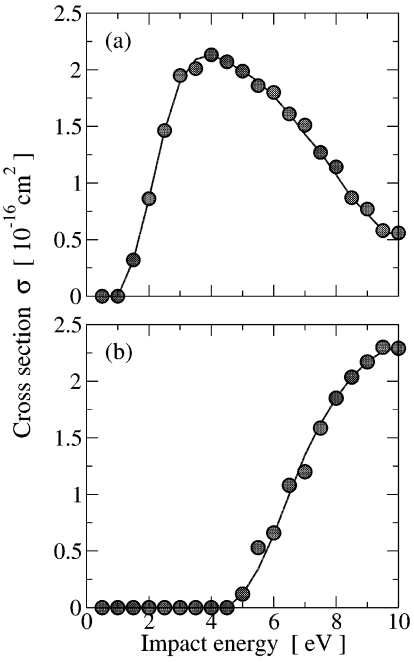

Figure 4. Calculated reaction cross sections σ as a function of relative impact kinetic energy for a thermal excitation of the H_2 reactants to 1000 K corresponding to $H_2(\nu_0{=}0,J_0{=}3)$: (a) for SiH^+ production and (b) for complete dissociation. The continuous lines only serve as a guide for the eye.

the hydrogen molecule at an infinite distance, we can express the energy balance for the creation of SiH^+ as follows:

$$-D_0(H_2) + E_{\nu_0,J_0} + E_0 = -D_0(SiH^+) + E_{\nu,J} + E_{rel} \quad (1)$$

where D_0 are the dissociation energies of 4.47 and 3.22 eV for H_2 and SiH^+, respectively,[18] E_{ν_0,J_0} is the initial ro-vibrational energy of the H_2 molecules, $E_{\nu,J}$ is the internal energy of the SiH^+ products, and E_{rel} is the relative translational energy between the separating products. Consequently, the energy available to the reaction products is

$$E_{\nu,J} + E_{rel} = D_0(SiH^+) - D_0(H_2) + E_{\nu_0,J_0} + E_0 \quad (2)$$

In the following, we will vary the collision energy E_0 from 0.5 to 10 eV to calculate reactive cross sections as well as rotational and vibrational energy distributions of the SiH^+ products.

3. Results

Donnelly et al. showed that by increasing the radio frequency power and the H_2 pressure, the plasma temperature can be increased to a maximum value of about 1000 K.[19] These extreme conditions result in higher film growth rates, which is one of the main challenges in the electronic industry. Consequently, we will begin our present study with experimental conditions similar to those where the H_2 molecule temperature is around 1000 K. The *most probable* values of the vibrational and rotational quantum numbers in a Boltzmann distribution at 1000 K are $\nu_0 = 0$ and a value slightly higher than $J_0 = 2$. The *average* rotational quantum number at this temperature, however, is close to $J_0 = 3$. Because we are interested in the maximum effect a realistic plasma heating to 1000 K might have on our title reaction, we chose the ($\nu_0 = 0$, $J_0 = 3$) state for the initial excitation of the hydrogen molecule. In Figure 4, we show how the reactive cross sections σ depend on the relative translational impact energy of the reactants. The maximum cross section for SiH^+ formation is now 2.2 Å^2 at approximatively 4 eV which, however, corresponds to an increase of only about 25% in comparison with the room temperature case. Increasing our present experimental plasma temperature of about 300 K to a temperature as high as 1000 K would consequently only result in a quite negligible increase in reactivity for the SiH^+ production.

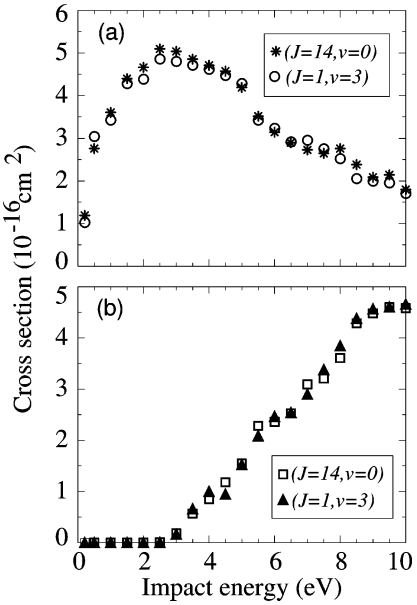

Figure 5. Calculated reaction cross sections σ as a function of relative impact kinetic energy for an initial laser excitation of the H_2 reactant to ($\nu_0 = 3$, $J_0 = 1$) and ($\nu_0 = 0$, $J_0 = 14$), both corresponding to an internal energy E_{int} of 1.8 eV (see text): (a) for SiH^+ production, $Si^+ + H_2(\nu_0,J_0) \rightarrow SiH^+(\nu,J) + H$, and (b) for complete dissociation, $Si^+ + H_2(\nu_0,J_0) \rightarrow Si^+ + H + H$.

Therefore, we will investigate in the following if selective laser excitation of the internal degrees of freedom could possibly result in a considerably higher increase of the reactive cross section. At room temperature, the reactive cross section increases from its minimum to its maximum value when the impact energy varies by about 1.8 eV. Therefore, we choose a laser excitation that roughly corresponds to an increase of internal energy of also about 1.8 eV. According to the chosen spectral transition, this energy allows us to either favor the rotational or the vibrational degree of freedom of the $H_2(\nu_0,J_0)$ reactants. Consequently, we will consider two distinct, initial quantum states for the hydrogen molecules: ($\nu_0 = 0$, $J_0 = 14$) and ($\nu_0 = 3$, $J_0 = 1$). Thus, we propose a crossed molecular beam experiment where rotationally and vibrationally cold hydrogen molecules are state-selectively excited with a laser prior to their interaction with silicon ions.

As shown in Figure 5a, the cross section of the $Si^+ + H_2 \rightarrow SiH^+ + H$ reaction now rises to a maximum of 4.8 Å^2 at 2.5 eV. Thereafter, the cross section again decreases due to the opening of the complete dissociation channel $Si^+ + H_2 \rightarrow Si^+ + H + H$ (see Figure 5b). The general shape of these two curves is very similar to that previously found for hydrogen at 1000 K and at room temperature.[8,10] In the present case with selective initial internal energy excitation of the reactant, however, the maximum SiH^+ cross section is about 3 times higher than in our previous investigation at room temperature. Besides, the threshold energies for both SiH^+ formation and complete dissociation are shifted by about 1.5 eV toward lower energies in comparison to those obtained for room temperature hydrogen $H_2(\nu_0{=}0,J_0{=}1)$. Those effects were entirely negligible in our above study at a temperature of 1000 K. Therefore, we will

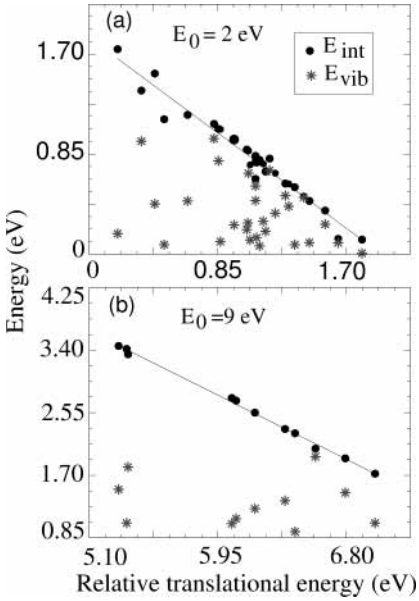

Figure 6. Internal and vibrational energy of $SiH^+(\nu,J)$ products as a function of relative translational product separation energy E_{rel} for two different impact energies E_0.

use the reactant preparation by laser excitation in the following to analyze the role of the initial internal energy for the dynamics of the title reaction in more detail. Figure 6 shows the evolution of the internal energy E_{int} for SiH^+ products as a function of the relative translational energy between the separating products for impact energies E_0 of 2 and 9 eV. These two different impact energies correspond respectively to indirect and direct scattering processes.[10,14] As demonstrated in these two figures, (a) and (b), the internal energy follows a straight line, as should be expected from energy conservation (see eq 2). We remind the reader that our data points for E_{int} scatter somewhat around the straight line because we randomly varied the impact energy by 10% for different trajectories (see section 2). The vibrational energy E_{vib} seems to be randomly distributed for both impact energies E_0. We have observed a very similar vibrational energy dependence in our previous studies without any H_2 internal energy excitation.[14]

To understand the behavior of the vibrational energy better, we determined the vibrational energy distributions of the SiH^+ products separately for initial vibrational, rotational, and translational excitation of the H_2 molecules. Examining the simulated trajectories in detail, we can clearly distinguish direct and indirect reactive scattering processes and analyze them separately. In Figure 7, we show the average lifetime τ of those SiH_2^+ complexes that result in SiH^+ production. For each impact energy, the half-width of the lifetime distribution corresponds to about 35% of the lifetime. The SiH^+ formation becomes entirely direct for impact energies exceeding 6 eV. We point out that the slope of the corresponding logarithmic display of the SiH^+ product resolved lifetimes indicates a barrier height of 2.2 eV. This energy barrier gives the energy necessary to overcome the complex to form the final SiH^+ product, in excellent agreement with the value we previously determined for hydrogen at room temperature.[10]

The SiH^+ vibrational energy distributions calculated for an initial internal excitation of the $H_2(\nu_0,J_0)$ molecule to ($\nu_0 = 3$, $J_0 = 1$) and ($\nu_0 = 0$, $J_0 = 14$) are displayed in Figure 8a−d for a collision energy of 2 eV. In panels e and f of this figure, we show the corresponding distributions for room temperature $H_2(\nu_0{=}0,J_0{=}1)$ molecules with an impact energy of 3.5 eV. This

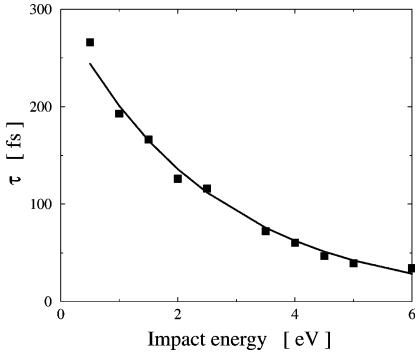

Figure 7. Calculated H_2Si^+ complex lifetime τ as a function of kinetic impact energy E_0 for complexes leading to SiH^+ formation. The continuous line corresponds to an exponential fit.

latter collision energy has been chosen in such a way that the available energy $E_{\nu,J} + E_{rel}$ as defined in the last section (see eq 2) takes the same value in all three cases. The upper panels show the vibrational energy distributions $P_{dir}(E_{vib})$ obtained only from direct reaction processes. In the lower panels, we display $P_{com}(E_{vib})$, resulting only from indirect complex-mediated processes. In the latter case, there are clearly two distinct distributions (see Figure 8b,d,f): one at lower vibrational energies (<0.8 eV) corresponding to a short-lived, loose complex formation and the other one at higher vibrational energies corresponding to more stable H_2Si^+ complexes. The short complex lifetimes do not exceed 80 fs, which only corresponds to a few vibrational periods of the SiH^+ molecule.[18] The resulting complex lifetime is hence too short to transfer a large amount of energy to the vibrational degree of freedom, as will be discussed below in more detail. Therefore, we propose to assign the low-energy distributions in Figure 8b,d,f rather to *quasi-direct* than complex-mediated processes. The involved energy transfer processes should, thus, be closely related to direct ones. The lifetimes τ corresponding to the second distributions around 1.8 eV are at least 5 times longer, permitting efficient energy transfer to the product vibration. Interestingly, the same vibrational energy distributions are obtained for different initial ro-vibrational and translational excitation states, as shown in Figure 8 for both direct and complex-mediated reaction paths.

Figure 9 presents the evolution of the vibrational energy of the SiH^+ products averaged separately for direct and indirect processes. The vibrational energy $\langle E_{vib}\rangle_{com}$ averaged only over trajectories involving an intermediate *three-atom-complex* (i.e., indirect processes) is shown in Figure 9a. The vibrational energy increases with impact energy until 4.5 eV and decreases thereafter. Figure 9b shows that the vibrational energy $\langle E_{vib}\rangle_{dir}$ averaged only over direct trajectories increases with impact energy until 6 eV, when it starts to "saturate" around 1.4 eV. Clearly, the product vibrational energies are considerably higher for the indirect, complex-mediated process than for the direct one. The vibrational energy $\langle E_{vib}\rangle$ averaged over both direct and indirect processes is shown in Figure 9c. For the latter $\langle E_{vib}\rangle$ calculations, we considered the respective probabilities for the two processes. In fact, $\langle E_{vib}\rangle$ increases until 6 eV, when it approaches a saturation value of about 1.4 eV.

The evolution of rotational E_{rot} and relative translational E_{rel} energies averaged separately over the two reaction paths are displayed in Figures 10 and 11, respectively. Again, there are two clearly distinct regions: one above and one below 6 eV. As will be discussed in the following section, this change in slope can be attributed to a transition from indirect to direct reaction processes.

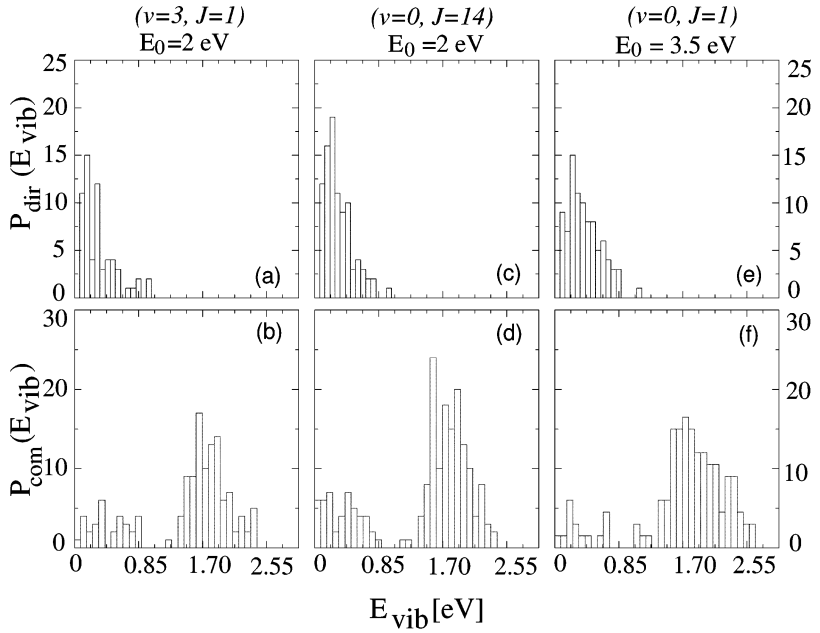

Figure 8. Vibrational energy E_{vib} distributions of the SiH^+ products: upper panels for SiH^+ formed through a direct reaction path, lower panels via a complex-mediated reaction path. The vertical scale represents the number of trajectories that led to SiH^+ production for different initial excitation states of the $H_2(v_0,J_0)$ reactant, all corresponding to a total energy of 3.8 eV: (a) and (b) ($v_0 = 3$, $J_0 = 1$) with 2 eV impact energy; (c) and (d) ($v_0 = 0$, $J_0 = 14$) with 2 eV impact energy; (e) and (f) ($v_0 = 0$, $J_0 = 1$) with 3.5 eV impact energy.

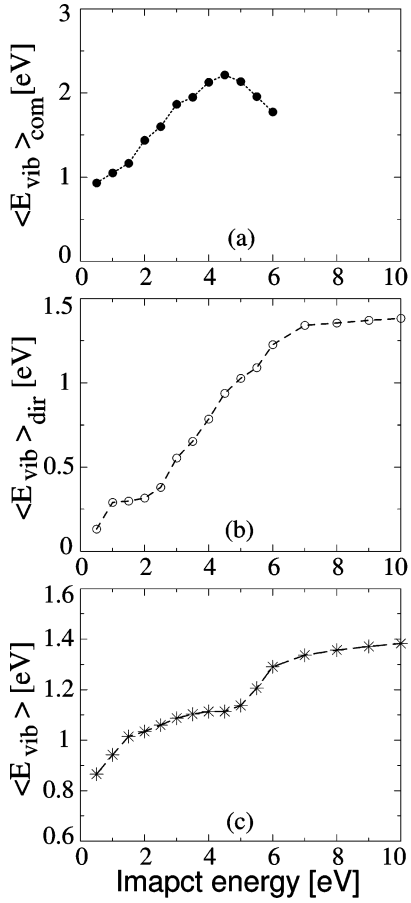

Figure 9. Averaged vibrational energies as a function of kinetic impact energy: (a) averaged only over indirect processes, (b) averaged only over direct processes, and (c) averaged over both possible reaction paths.

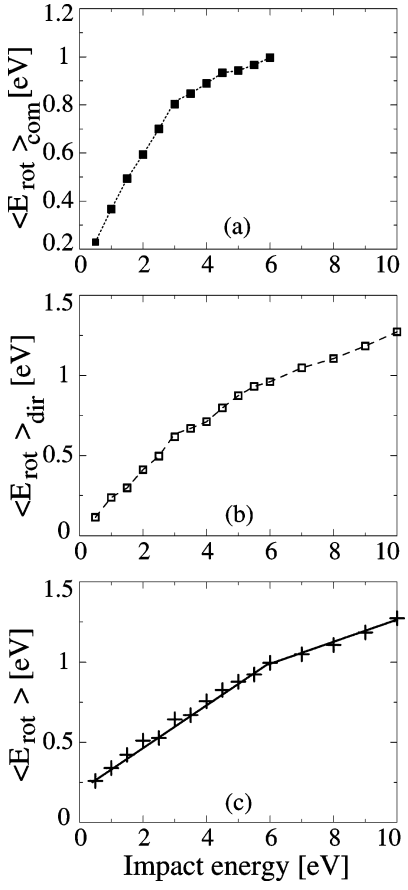

Figure 10. Averaged rotational energies as a function of kinetic impact energy and reaction paths: (a) averaged only over indirect processes, (b) averaged only over direct processes, and (c) averaged over both possible reaction paths.

4. Discussion

We showed that thermal heating of the hydrogen gas to a temperature as high as 1000 K increases the reactive cross section for SiH^+ formation by only 25%. Consequently, we explored the use of selective laser excitation of the hydrogen reactants and we demonstrated that such a preparation scheme can drastically enhance the reactivity of our system. In Figure 5a, the reactive cross section for SiH^+ production strongly

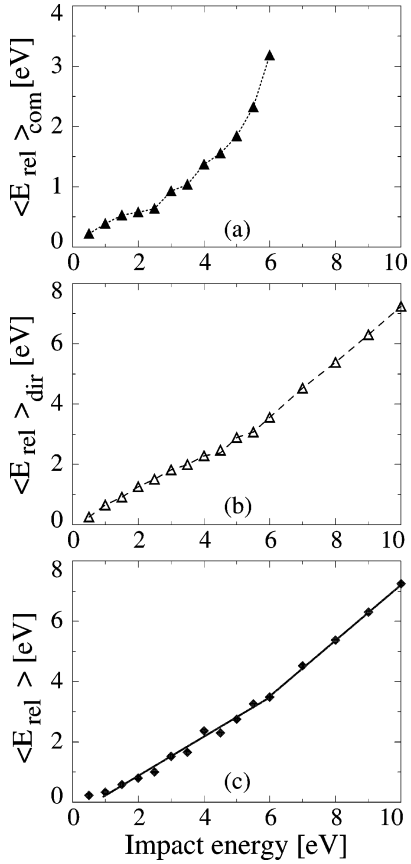

Figure 11. Averaged translational product separation energies as a function of kinetic impact energy: (a) averaged only over indirect processes, (b) averaged only over direct processes, and (c) averaged over both possible reaction paths.

depends on the energy of the incoming particles and has a maximum of 4.8 Å^2 at 2.5 eV. This maximum cross section resulting from internally excited H_2 reactants is about 3 times higher than the one previously determined for room temperature hydrogen.[8,10] This behavior clearly demonstrates that the internal reactant energy enhances the reactivity of our system much more efficiently than the translational impact energy. This important result has previously been observed experimentally for initial electronic excitation of one of the reactants for Cs + H_2 reactive scattering where the cross section σ [Cs($^7P_{1/2}$)] is 4 times higher than σ [Cs($^7P_{3/2}$)].[20] Moreover, the cross sections for H_2 molecules initially in their ($v_0 = 3$, $J_0 = 1$) or ($v_0 = 0$, $J_0 = 14$) states show the same variation with kinetic impact energies. Consequently, both initial excitation states equally enhance the reactivity of our system despite the fact that vibrational energy is often considered the crucial energy form to favor chemical reactions. The present results show that the three atoms "lose the memory" of their initial conditions when they interact, as will be further discussed in the following.

Further comparing our present results with previous room temperature calculations, we find that the maximum SiH^+ cross section is shifted by about 1.5 eV toward lower collision energies for reactants with increased internal energy. This energy amount roughly corresponds to the difference in initial internal energy excitation of the $H_2(v_0,J_0)$ molecules (i.e., $E_{(v_0=3,J_0=1)} - E_{(v_0=0,J_0=1)} = 1.5$ eV). In the same sense, the calculated cross section for the complete dissociation channel has now a threshold of about 3 eV (see Figure 5b). This threshold energy is again about 1.5 eV lower than in the case where the H_2 molecules are at 305 K ($v_0 = 0$, $J_0 = 1$) where complete dissociation only starts to take

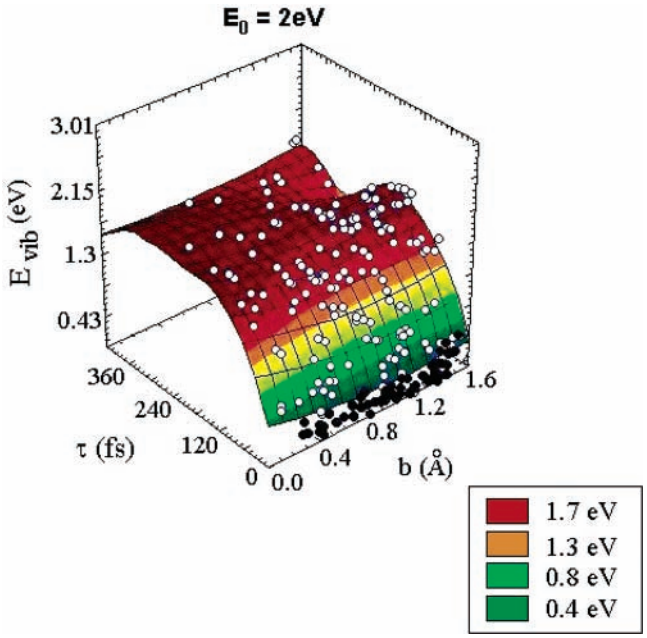

Figure 12. Correlation between vibrational energy E_{vib}, impact parameter b, and complex lifetimes τ for SiH^+ products.

place above $D_0(H_2) = 4.5$ eV.[8] For the laser excitation conditions ($E_{int} = 1.8$ eV), this threshold is lowered by the difference in initial internal energy of the H_2 reactants. In our study of a thermal excitation of the hydrogen gas to 1000 K such a shift is too small to be detected; i.e., the internal energy difference is not sufficient to cause a significant shift in the reaction threshold.

We now turn our attention to the mechanisms of vibrational, rotational, and translational energy transfer in the reactive scattering processes of Si^+ with H_2. As shown in Figure 6, we have investigated the SiH^+ internal E_{int} and vibrational E_{vib} energy dependence on the relative translational product separation energy E_{rel} for two different impact kinetic energies. The vibrational energy seems to be randomly distributed for both impact energies, which is not the case for the total internal energy E_{int} that follows a linear dependence with E_{rel}, as expected for energy conservation. One might consequently ask if this randomness represents the true nature of the investigated reactive scattering or if it simply results from our simulation method; i.e., the impact parameter b is randomly chosen in our molecular dynamic simulations, which might intuitively influence the reaction dynamics. Figure 12 shows the vibrational product energy as a function of both impact parameter b and complex lifetime τ for an impact energy of 2 eV. The vibrational energy turns out to be largely independent of the impact parameter b, whereas it shows a clear increase with the complex lifetime τ. There is no sign of vibrational energy dependence on the impact parameter either for indirect or for direct processes; the latter ones are represented by black circles situated at the lowest vibrational energies. Therefore, we propose that the vibrational energy transfer becomes clearly enhanced with increasing lifetime of the SiH_2^+ intermediate complex. This result is in excellent agreement with our previous findings shown in Figure 8, where the highest vibrational energy transfer is obtained for longer complex lifetimes corresponding to the second distribution as shown in the lower panels (see Figure 8b,d,f).

One question which remains is why the vibrational energy distribution versus E_{rel} presents the same random behavior also at $E_0 = 9$ eV (see Figure 6). At 9 eV impact energy, the SiH^+ production is completely direct and there is no more intermediate

complex formation favoring the vibrational energy transfer. Accordingly, we again analyzed the evolution of E_{vib} and E_{rot} as function of b, but we could not find any correlation. Consequently, the redistribution of internal energy over rotation and vibration appears simply random at 9 eV. This observation is in accordance with the "lost memory" hypothesis suggested by Bonnet et al.[21] This idea is further supported by our observation that the E_{vib} distributions at 9 eV present the same behavior for excitation of the vibrational, the rotational, or the translational degree of freedom. Indications for such strong three-body interactions was previously suggested by Mahan et al. for the dynamics of the C^+ with H_2 reaction.[22]

To understand the underlying Si^+ and H_2 scattering dynamics better, we analyzed our results separately for direct and indirect reaction paths. We tentatively attributed the decrease of the averaged vibrational energy above 4 eV (see Figure 9a) to the decrease of the complex lifetime as a function of impact energy, as shown in Figure 7. The SiH^+ formation becomes entirely direct for impact energy exceeding 6 eV. This energy is again about 1.5 eV lower than the value we found for H_2 molecules at room temperature.[14] Increasing the impact energy beyond 7 eV, we find that the vibrational SiH^+ product energy remains roughly constant around 1.4 eV, as shown in Figure 9b,c. This observation can probably be understood by the high internal energy of the SiH^+ molecules; i.e., $\langle E_{int}\rangle = \langle E_{vib}\rangle + \langle E_{rot}\rangle$ is about 2.3 eV for $E_0 = 6$ eV (see Figures 9c and 10c). Consequently, the SiH^+ dissociation energy of 3.2 eV can readily be reached considering that the width of the internal energy distribution ΔE_{int} is about ± 0.9 eV, as can be seen in Figure 6; i.e., above an impact energy of 6 eV, a further increase in vibrational energy leads more and more to dissociation of the SiH^+ products due to the violence of the direct reaction channel.

Concerning the rotational energies of the SiH^+ products, we note a clear dependence on the kinetic collision energy. The averaged rotational energy linearly increases with impact energy. However, there are clearly two distinct regions: one above and one below about 6 eV (see Figure 10c). The change in slope at 6 eV can be attributed to the transition from indirect to direct reaction mechanisms. As can be concluded from the respective slopes for both mechanisms, the efficiency of translational to rotational energy transfer is higher when mediated by the intermediate complex, but not as high as for the vibrational energy transfer. Comparing Figure 10a,b, we can note that the rotational energies have the same order of magnitude for indirect and direct processes until 6 eV impact energy, which is not the case for the vibrational energies (see Figure 9a,b). In this latter case, the averaged vibrational energies $\langle E_{vib}\rangle_{com}$ for the indirect process is 2 times higher than for the direct one, suggesting a strong transfer enhancement due to the intermediate complex formation. In other words, the rotational degree of freedom experiences less enhancement from the intermediate complex than the vibrational one because the SiH^+ product cannot rotate freely in the intermediate complex because it is hindered due to collisions with the remaining H atom. The dynamical reason for this is that the typical motion of the triatomic complex is *vibration* involving all three atoms equally, and not the hindered rotation of a diatom with respect to the third atom. This view has been previously discussed by Brass et al.[23] who showed that the inclusion of the vibrational degree of freedom is essential, if one wants to make a realistic model of a long-lived molecular complex.

We easily distinguish also two different regions for the translational energy dependence: one below and one above 6 eV, characterizing again direct and indirect reaction paths, respectively (see Figure 11c). For kinetic impact energies above 6 eV, the energy transfer to the translational degree of freedom gets more efficient than the transfer to the rotational or vibrational ones. Consequently, less energy is left for the internal degrees of freedom, which is in excellent agreement with our findings relative to the vibrational and rotational energy distributions, especially for E_{vib} that *saturates* for this range of E_0 because the vibrational energy transfer takes more time than the rotational and especially than the translational one.

5. Conclusion

We studied how the reactive scattering dynamics is influenced by vibrational and rotational excitation of molecular hydrogen prior to its interaction with silicon ions. Using semiempirical quantum molecular dynamics, we demonstrated that the reactivity between $H_2(v_0,J_0)$ and $Si^+(^2P)$ becomes enhanced by the prior internal energy excitation of the hydrogen molecules.

We showed that thermal heating of our plasma from 300 to 1000 K will only result in a very minor increase of the maximum reactive cross section by about 25%. Because a temperature of 1000 K rather represents a maximum value for possible plasma heating in our reactors, we explored the influence of a possible laser excitation of the $H_2(v_0,J_0)$ reactants. In this case, we demonstrated that both the absolute amplitude of the reactive cross section and the shift of its maximum toward lower impact energies only depend on the *amount* of initial internal excitation and not on its precise *nature*; i.e., initial *rotational* excitation enhances the reactivity of our system in the same way as prior *vibrational* excitation.

At impact energies lower than 6 eV, the scattering dynamics is governed by intermediate complex mediated processes, whereas direct mechanisms become predominant at higher translational collision energies. For the latter, the most efficient energy transfer channel is clearly from the impact kinetic energy of the reactants to the relative translational energy with which the products separate. Although there is still also some energy transfer to the rotational energy of the SiH^+ products at those high collision energies, the product vibrational energy saturates above 6 eV. For impact energies below 6 eV, on the other hand, we showed that the temporary formation of an intermediate three-atom-complex clearly favors the energy transfer toward the vibrational degree of freedom of the SiH^+ products. Notably, we illustrated that the amount of vibrational energy transferred to the SiH^+ product is clearly determined by the lifetime of the intermediate complex.

Acknowledgment. This work has been partially financed by the "French Ministére de Recherche" in the framework of the program "ACI Nanostructures" under the contract No. N52-01 and by research grants from the Natural Science and Engineering Research Council (NSERC) of Canada. Most of the calculations were performed at the French National Computer Center IDRIS. Some of the initial calculations were carried out at the Centre for Research in Molecular Modeling CERMM in Montréal. We acknowledge the computer time that was allotted for the present study by both IDRIS and CERMM. We also thank those at the computer center of Ecole Polytechnique (DSI) who helped us to complete the current work. Finally, we acknowledge many fruitful discussions with Professor Gilles Ohanessian and Professor Pascal Le Floch at the Ecole Polytechnique.

References and Notes

(1) Ervin, K. M.; Armentrout, P. B. *J. Chem. Phys.* **1986**, *84*, 6738.

(2) Varley, D. F.; Levandier, D.; Farrar, J. *J. Chem. Phys.* **1992**, *96*, 8806.
(3) Qian, J.; Green, R. J.; Anderson, S. L. *J. Chem. Phys.* **1998**, *108*, 7173.
(4) L'Hermit, J. M.; Rahmat, G.; Vetter, R. *J. Chem. Phys.* **1990**, *93*, 434.
(5) Cavero, V.; L'Hermite, J. M.; Rahmat, G.; Vetter, R. *J. Chem. Phys.* **1998**, *110*, 3428.
(6) Scheier, P.; Marsen, B.; Lonfat, M.; Schneider, W. D. *Surf. Sci.* **2000**, *458*, 113.
(7) Maus, M.; Gantefor, G.; Eberhardt, W. *Appl. Phys. A* **2000**, *70*, 535.
(8) Elkind, J. L.; Armentrout, P. B. *J. Phys. Chem.* **1984**, *88*, 5454.
(9) Carlson, T. A.; Copley, J.; Duric, N.; Elander, N.; Larsson, M.; Lyyra, M. *Astron. Astrophys.* **1980**, *83*, 238.
(10) Vach, H.; Chaâbane, N.; Peslherbe, G. H. *Chem. Phys. Lett.* **2002**, *352*, 127.
(11) Chaâbane, N.; Vach, H.; Peslherbe, G. H. *Technol. Proc Int. Conf. Modeling Simulation Microsystems, 4th* **2001**, *4*, 434.
(12) Stewart, J. J. P. *J. Comput. Chem.* **1989**, *10*, 209.
(13) Stewart, J. J. P. *J. Comput. Chem.* **1989**, *10* 221.
(14) Chaâbane, N.; Vach, H.; Peslherbe, G. H. *J. Non-Cryst. Solids* **2002**, *299*−*302*, 42.
(15) Frisch, M. J.; Trucks, G. W.; Schlegel, H. B.; Scuseria, G. E.; Robb, M. A.; Cheeseman, J. R.; Zakrzewski, V. G.; Montgomery, J. A., Jr.; Stratmann, R. E.; Burant, J. C.; Dapprich, S.; Millam, J. M.; Daniels, A. D.; Kudin, K. N.; Strain, M. C.; Farkas, O.; Tomasi, J.; Barone, V.; Cossi, M.; Cammi, R.; Mennucci, B.; Pomelli, C.; Adamo, C.; Clifford, S.; Ochterski, J.; Petersson, G. A.; Ayala, P. Y.; Cui, Q.; Morokuma, K.; Malick, D. K.; Rabuck, A. D.; Raghavachari, K.; Foresman, J. B.; Cioslowski, J.; Ortiz, J. V.; Stefanov, B. B.; Liu, G.; Liashenko, A.; Piskorz, P.; Komaromi, I.; Gomperts, R.; Martin, R. L.; Fox, D. J.; Keith, T.; Al-Laham, M. A.; Peng, C. Y.; Nanayakkara, A.; Gonzalez, C.; Challacombe, M.; Gill, P. M. W.; Johnson, B. G.; Chen, W.; Wong, M. W.; Andres, J. L.; Head-Gordon, M.; Replogle, E. S.; Pople, J. A. *Gaussian 98*, revision x.x; Gaussian, Inc.: Pittsburgh, PA, 1998.
(16) Hase, W. L.; Duchovic, R. J.; Hu, X.; Komornicki, A.; Lim, K. F.; Lu, D.; Peslherbe, G. H.; Swamy, K. N.; Vande Linde, S. R.; Varanda, A.; Haobin, W.; Wolf, R. J. *VENUS96: General Chemical Dynamics Computer Program*; Department of Chemistry, Wayne State University: Detroit, MI, 1996.
(17) Press, W. H.; Vetterlin, W. T.; Teukolsky, S. A.; Flannery, B. P. *Numerical Recipes in Fortran: The Art of Scientific Computing*; Cambridge University Press: Cambridge, U.K., 1992.
(18) Herzberg, G. *Molecular Spectra and Molecular Structure: I. Spectra of Diatomic Molecules*; D. van Nostrand Co., Inc.: Princeton, NJ, 1966.
(19) Donnelly, V.; Flamm, D.; Collins, G. *J. Vac. Sci. Technol.* **1982**, *21*, 817.
(20) L'Hermite, J. M.; Rahmat, G.; Vetter, R. *J. Chem. Phys.* **1991**, *95*, 3347.
(21) Bonnet, L.; Rayez, J. C.; Halvick, P. *J. Chem. Phys.* **1993**, *99*, 1771.
(22) Mahan, B. H.; Sloane, T. M. *J. Chem. Phys.* **1973**, *59*, 5661.
(23) Brass, O.; Schlier, C. *J. Chem. Phys.* **1988**, *88*, 935.